



Hardware Implementation and Market Impacts of Grid-Supportive Functions in End-Use Loads

Yeongrack Son,¹ Sunil Subedi,^{1,2} Michael Blonsky,¹ and Barry Mather¹

1 National Renewable Energy Laboratory

2 South Dakota State University

**NREL is a national laboratory of the U.S. Department of Energy
Office of Energy Efficiency & Renewable Energy
Operated by the Alliance for Sustainable Energy, LLC**

This report is available at no cost from the National Renewable Energy Laboratory (NREL) at www.nrel.gov/publications.

Contract No. DE-AC36-08GO28308

Technical Report
NREL/TP-5D00-85188
March 2023



Hardware Implementation and Market Impacts of Grid-Supportive Functions in End-Use Loads

Yeongrack Son,¹ Sunil Subedi,^{1,2} Michael Blonsky,¹ and Barry Mather¹

1 National Renewable Energy Laboratory

2 South Dakota State University

Suggested Citation

Son, Yeongrack, Sunil Subedi, Michael Blonsky, and Barry Mather. 2023. *Hardware Implementation and Market Impacts of Grid-Supportive Functions in End-Use Loads*. Golden, CO: National Renewable Energy Laboratory. NREL/TP-5D00-85188. <https://www.nrel.gov/docs/fy23osti/85188.pdf>.

**NREL is a national laboratory of the U.S. Department of Energy
Office of Energy Efficiency & Renewable Energy
Operated by the Alliance for Sustainable Energy, LLC**

This report is available at no cost from the National Renewable Energy Laboratory (NREL) at www.nrel.gov/publications.

Contract No. DE-AC36-08GO28308

Technical Report
NREL/TP-5D00-85188
March 2023

National Renewable Energy Laboratory
15013 Denver West Parkway
Golden, CO 80401
303-275-3000 • www.nrel.gov

NOTICE

This work was authored in part by the National Renewable Energy Laboratory, operated by Alliance for Sustainable Energy, LLC, for the U.S. Department of Energy (DOE) under Contract No. DE-AC36-08GO28308. Funding provided by the U.S. Department of Energy Office of Energy Efficiency and Renewable Energy Strategic Analysis Team and the Building Technologies Office. The views expressed herein do not necessarily represent the views of the DOE or the U.S. Government.

This report is available at no cost from the National Renewable Energy Laboratory (NREL) at www.nrel.gov/publications.

U.S. Department of Energy (DOE) reports produced after 1991 and a growing number of pre-1991 documents are available free via www.osti.gov.

Cover Photos by Dennis Schroeder: (clockwise, left to right) NREL 51934, NREL 45897, NREL 42160, NREL 45891, NREL 48097, NREL 46526.

NREL prints on paper that contains recycled content.

Acknowledgments

This work was supported by the U.S. Department of Energy Office of Energy Efficiency and Renewable Energy Strategic Analysis Team and the Building Technologies Office. We especially thank Sam Baldwin and Wyatt Merrill for their support, feedback, and continued interest in this work. We also thank David Holmburg, Paul Denholm, Vahan Gevorgian, Killian McKenna, Andy Hoke, and Rasel Mahmud for providing their review and feedback on this report.

List of Acronyms

ADC	analog-to-digital converter
BOM	bill of materials
DER	distributed energy resource
ERCOT	Electric Reliability Council of Texas
EV	electric vehicle
FFR	fast frequency response
FRR	frequency response requirement
GSL	grid-supportive load
HVAC	heating, ventilating, and air conditioning
IEEE	Institute of Electrical and Electronics Engineers
IFRO	Interconnection Frequency Response Obligation
LED	light-emitting diode
MCU	microcontroller unit
NREL	National Renewable Energy Laboratory
PLL	phase-locked loop
PV	photovoltaics
VFD	variable-frequency drive
VRE	variable renewable energy
ZCD	zero-crossing detection

Executive Summary

Future power systems will see a marked increase in the incorporation of power electronics-based resources. These resources will include variable renewable energy sources, such as solar photovoltaics and wind; battery energy storage; and end-use loads, including electric vehicles (EVs) and electric motors with variable-frequency drives. Although power electronics-based resources provide the electric grid with renewable generation and efficient end-use equipment, they pose difficulties in maintaining grid stability because of a significant decrease in system inertia. A low-inertia power system is likely to experience more severe grid frequency variations in the case of a sudden shift in supply or demand. Additional frequency response is required to mitigate these variations and maintain grid stability.

Grid-supportive loads (GSLs) are power electronics-based end-use loads that can provide frequency response and other grid services by autonomously adjusting their output power using local grid measurements. During a low-frequency event, GSLs can measure the frequency locally and quickly reduce their energy consumption for a short time to raise the frequency nadir as shown in Figure ES-1. Their autonomous control also reduces cybersecurity-related concerns. GSLs can be a cost-effective option for frequency response in a low-inertia grid because they have low operational costs relative to other resources and have minimal impact on the end user.

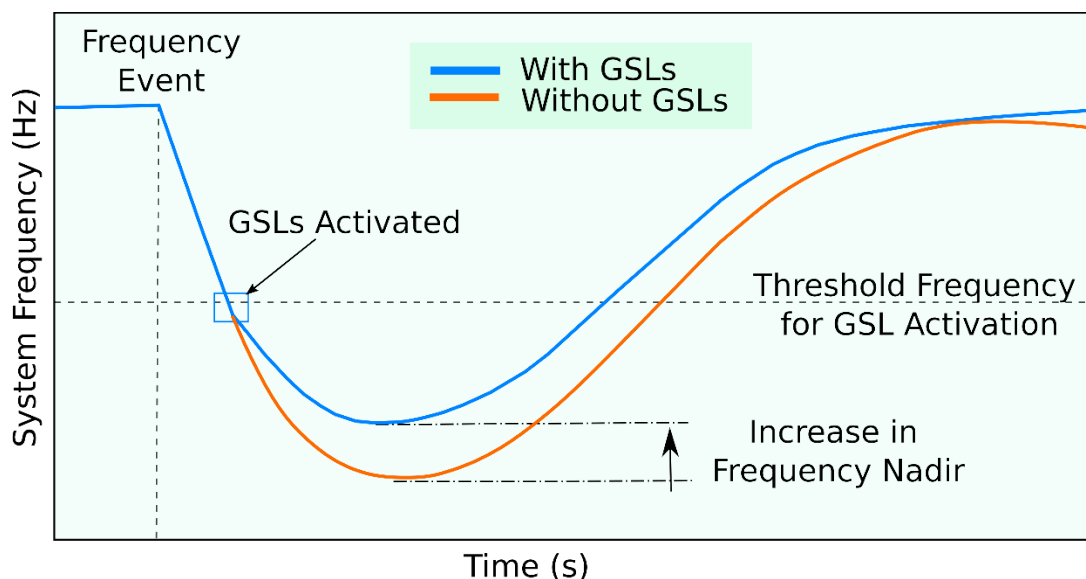


Figure ES-1. Impact of GSLs on frequency nadir

This report describes hardware designs and hardware costs to implement GSL functions in end-use loads. Multiple hardware designs are analyzed for single- and three-phase devices. We assess each design in terms of materials, costs, and impacts on isolation and microcontroller requirements, and we estimate the energy consumption associated with GSL functionality. We find that the most cost-effective design costs \$1.15 for single-phase loads and \$2.46 for three-phase loads. An increase in standby losses leads to additional energy consumption costs of approximately \$1.

If implemented at scale, GSLs can provide a significant amount of the current frequency response requirements in U.S. grids. Millions of refrigerators, EV chargers, or residential heat

pumps would be required to meet 100% of the current national requirement, which is feasible given the number of available devices projected to be on the grid in the near future. We list the technical and market barriers associated with GSLs, and we describe multiple adoption pathways to mitigate these barriers and encourage GSL growth.

Given the rapidly changing mix of electric grid generators and loads, it is difficult to predict whether GSLs will be a cost-effective resource for frequency response and other grid services. Hardware testing and pilot programs will help define the set of costs and benefits that GSLs can provide to grid operators, manufacturers, and energy consumers.

Table of Contents

1	Introduction	1
1.1	Resources for Up-Frequency and Down-Frequency Response.....	2
1.2	Frequency Response in Low-Inertia Systems.....	3
2	Implementation of Grid-Supportive Load Functions	5
2.1	Line Voltage Scaling.....	6
2.2	Signal Isolation.....	7
2.3	Frequency Detection.....	8
2.4	Grid-Supportive Load Control Implementation.....	9
2.5	Grid-Supportive Load Hardware Design Classification.....	10
3	Grid-Supportive Load Implementation Costs	13
3.1	Hardware Costs.....	13
3.2	Cost-Effective Designs for End-Use Equipment.....	18
4	Market Impacts of Grid-Supportive Loads	21
4.1	Grid-Supportive Load Adoption Pathways.....	21
4.2	Meeting Frequency Response Requirements.....	22
5	Conclusion	26
	References	27

List of Figures

Figure ES-1. Impact of GSLs on frequency nadir.....	v
Figure 1. Impact of GSLs on frequency nadir	4
Figure 2. Block diagram of GSL hardware and firmware implementation	5
Figure 3. Line voltage scaling circuit with a voltage divider.....	6
Figure 4. Line voltage scaling circuit with a shunt resistor	6
Figure 5. PLL block diagram for three-phase line-connected load.....	9
Figure 6. Conceptual diagrams of the ZCD method using the time between pulses (left) and the number of zero crossings between the fixed time period (right)	9
Figure 7. Frequency-watt curve for GSL control implementation.....	10
Figure 8. Type I design: non-isolated design with voltage divider.....	11
Figure 9. Type II design: isolated design with voltage divider and analog output	11
Figure 10. Type III design: isolated design with voltage divider and digital output	11
Figure 11. Type IV design: isolated design with current-limiting resistor and analog output.....	12
Figure 12. Type V design: isolated design with current-limiting resistor and digital output.....	12
Figure 13. Common topology of a power electronics-based residential refrigerator with optional GSL hardware.....	19
Figure 14. Common topology of an EV charger with optional GSL hardware	20
Figure 15. Baseline load profile estimation of Level 2 and Level 3 EV chargers by 2030 in (a) Texas and (b) the contiguous United States	25

List of Tables

Table 1. Operational and Capital Costs for Up-Frequency and Down-Frequency Response Services	3
Table 2. Cost-Effective MCUs With Internal ADC Block	14
Table 3. BOM and Cost Estimates for Single-Phase Type I Design	14
Table 4. BOM and Cost Estimates for Single-Phase Type II Design	15
Table 5. BOM and Cost Estimates for Single-Phase Type III Design.....	16
Table 6. BOM and Cost Estimates for Single-Phase Type IV Design.....	17
Table 7. BOM and Cost Estimates for Single-Phase Type V Design.....	17
Table 8. Summary of the Cost Estimates for the Five Hardware Designs.....	18
Table 9. Number of GSL Devices Available and Required to Meet Current FRRs for ERCOT and Across the United States	24

1 Introduction

Future power systems will see a marked increase in the incorporation of power electronics-based resources. These resources will include variable renewable energy (VRE) sources, such as solar photovoltaics (PV) and wind; battery energy storage; and end-use loads, including electric vehicles (EVs) and electric motors with variable-frequency drives (VFDs) (Denholm, Sun, and Mai 2019). Although power electronics-based resources provide the electric grid with renewable generation and efficient end-use equipment, they pose difficulties in maintaining grid stability because of a significant decrease in system inertia (Chakravorty, Chaudhuri, and Hui 2017). A low-inertia power system is likely to experience more severe grid frequency variations in the case of a sudden shift in supply or demand (Ela, Hytowitz, and Helman 2019). Additional frequency response is required to mitigate these variations and maintain grid stability.

Gas-fired combustion turbines have historically provided frequency response to support the grid during contingency events, but these units are increasingly being replaced because of increasing operating costs and environmental concerns. More recently, batteries and other inverter-based resources have provided these services via fast frequency response (FFR) (Chakravorty, Chaudhuri, and Hui 2017). FFR combines inertia-like and primary contingency reserve characteristics by slowing the rate of change of frequency and increasing the frequency nadir during a contingency event. Nonsynchronous VRE sources can also provide FFR if they are designed to do so. As wind and PV integration increases, VRE sources are possible candidates for FFR, but they are better suited for events when the grid frequency is too high and the generation must be reduced. Up-frequency response (i.e., increasing generation or decreasing load in response to a low grid frequency) is challenging for VRE generators because it requires continuous real power curtailment to provide headroom such that extra power can be generated during a low-frequency event.

Loads can also provide up-frequency response because they are capable of temporarily reducing power use during low-frequency events (Anderson, Reilly, and Krishnan 2022). Large industrial load shedding has been implemented in several North American grids (Denholm, Sun, and Mai 2019). Frequency response from aggregations of smaller loads has been shown to be technically feasible with fast response times (Nandanoori et al. 2018). FFR in power electronics-based loads has also been tested in a large-scale laboratory setting (Lundstrom, Patel, and Salapaka 2021). These loads—especially VFDs—have been increasingly used to improve the efficiency and performance of commercial and industrial applications during the past decades (Rao et al. 2021). In residential settings, VFDs and DC motors are becoming more common in heating, ventilating, and air-conditioning (HVAC) equipment; refrigerators; and other appliances.

Grid-supportive loads (GSLs) can provide FFR with minimal impact on users. GSLs are power electronics-based end-use loads that are automatically and autonomously controlled based on local grid measurements, including voltage and frequency. During a low-frequency event, GSLs can measure the frequency locally and reduce their energy consumption for a short time to increase the frequency nadir. Additionally, some GSLs can provide local voltage regulation, power factor correction, and other ancillary services. Their autonomous control also reduces cybersecurity-related concerns. A study on a 2,000-bus feeder of the Texas power system demonstrated that 20% of all loads with GSL capabilities can increase the frequency response by

up to 2,000 MW/0.1 Hz and can reduce variance in the frequency nadir by up to 60% (Jain et al. 2022). Recent research has shown that multiple end-use applications have the technical potential for FFR (Blonsky, Subedi, and Mather 2022). An economic assessment showed that the FFR benefits of GSLs can outweigh their costs of implementation (Subedi et al. 2023).

This report presents research on the hardware implementation and market impacts of GSL functionality in end-use loads. The remainder of this section describes the resources available for up- and down-frequency response and the need for frequency response in low-inertia systems. Section 2 provides details on hardware implementation options and their impacts on GSL functionality. Section 3 presents hardware costs for these options and includes cost-effective designs for specific end-use technologies, including EV chargers, heat pumps, and refrigerators. Section 4 describes pathways for the market adoption of GSLs and their ability to meet current frequency response requirements.

1.1 Resources for Up-Frequency and Down-Frequency Response

Up-frequency response is the ability to increase generation or decrease load in response to a low-frequency event. Conversely, down-frequency response is the ability to reduce generation or increase load in response to a high-frequency event. To provide frequency response, a device must respond very quickly, e.g., within one second or less.

The following resources can provide frequency response, but they have different operational and capital costs as shown in Table 1:

- VRE sources can provide up-frequency response by maintaining headroom, but this is often undesirable due to economic loss from curtailment.¹ Down-frequency response is much more cost-effective for VRE sources because it only reduces generation during high-frequency events, which are very short and infrequent.
- Combustion turbines can provide up-frequency response and down-frequency response, but they can be more expensive and more polluting than other resources. Providing frequency response also reduces their capacity to provide other grid services, e.g., regulation and ramping services.
- Batteries are becoming more common for frequency response according to the U.S. Energy Information Agency (McGrath 2021). Similar to combustion turbines, providing frequency response reduces the battery's capacity to provide other grid services.
- Industrial load shedding can provide up-frequency response by shutting off large loads, which can lead to economic loss to the customer. The activation threshold for underfrequency load shedding is usually low to avoid frequency load-shedding events.
- GSLs can provide up-frequency response with very minimal operational costs due to negligible discomfort or inconvenience to the customer, e.g., needing a few more seconds to fully charge an EV; however, GSLs have higher capital costs because the frequency response controls must be installed on millions of devices. GSLs can also provide down-

¹ Studies have shown that wind turbines can provide up-frequency response without any headroom by extracting stored kinetic energy from the rotating blades (Denholm et al. 2020).

frequency regulation if they are not operating at full capacity; however, this might only be desirable for certain end uses, e.g., HVAC and refrigeration.

Table 1. Operational and Capital Costs for Up-Frequency and Down-Frequency Response Services

Resource	Up-Frequency Costs	Down-Frequency Costs	Capital Costs	Challenges With Up-Frequency
PV and wind (VRE)	Curtailment	Reduced energy	Added controls	<ul style="list-style-type: none"> Headroom requires continuous curtailment for up-frequency
Combustion turbines	Reduced capacity	Reduced capacity	Added controls	<ul style="list-style-type: none"> Low efficiency Reduction in power capacity for other services
Batteries	Reduced capacity	Reduced capacity	Added controls	<ul style="list-style-type: none"> Reduction in power capacity for other services Potential impact on degradation
Load shedding	Loss of service	N/A	Added controls	<ul style="list-style-type: none"> Economic loss Limited flexibility
GSLs	Reduced energy	Increased energy	Added hardware with controls	<ul style="list-style-type: none"> Negligible inconvenience for occupant/customer

Note: The colors indicate the relative average costs of frequency regulation for each resource. We note that costs can depend on the resource technology and the resource owner's willingness to provide grid services.

In a future low-carbon grid with many VRE sources and limited firm capacity from fossil-fueled plants, GSLs could be one of the most cost-effective options for up-frequency response. VRE sources can efficiently provide down-frequency response, but they will only be economic to provide up-frequency response during times of excess renewable generation. Batteries and generators with firm capacity will be needed for flexibility and ramping services, and providing frequency response would reduce their available capacity for those services. Underfrequency load shedding is still a viable option for up-frequency response, but the loss of load can lead to economic losses due to limited flexibility for most large loads. In contrast, GSLs are designed to have a much smaller impact on the customer and could be more frequently activated than industrial load shedding.

An additional benefit of GSLs is their ability to be used in microgrids when isolated from the bulk power system. Any GSLs that are located within a microgrid can provide up-frequency response regardless of whether the microgrid is connected or isolated. This reduces the need for the microgrid generator to provide these services and could reduce costs for microgrid operation.

1.2 Frequency Response in Low-Inertia Systems

Future grids will have less inertia as synchronous machines are replaced with inverter-based resources. One study finds that a 10% increase in VRE generation (from 20% to 30%) leads to a 10% decrease in average inertia and a 30% decrease in minimum inertia (Johnson, Rhodes, and Webber 2020). The minimum inertia occurs during times of low net load (i.e., load minus VRE generation), when most synchronous generators are off. Due to the high rate of change of

frequency in a low-inertia grid, more frequency response is required to increase the frequency nadir and prevent underfrequency load-shedding events and cascaded problems.

GSLs can provide FFR to increase the frequency nadir, as shown in Figure 1. GSLs can provide this type of fast power injection within the necessary time frames to avoid underfrequency load-shedding activation. We note that additional resources are required to restore system frequency to nominal values.

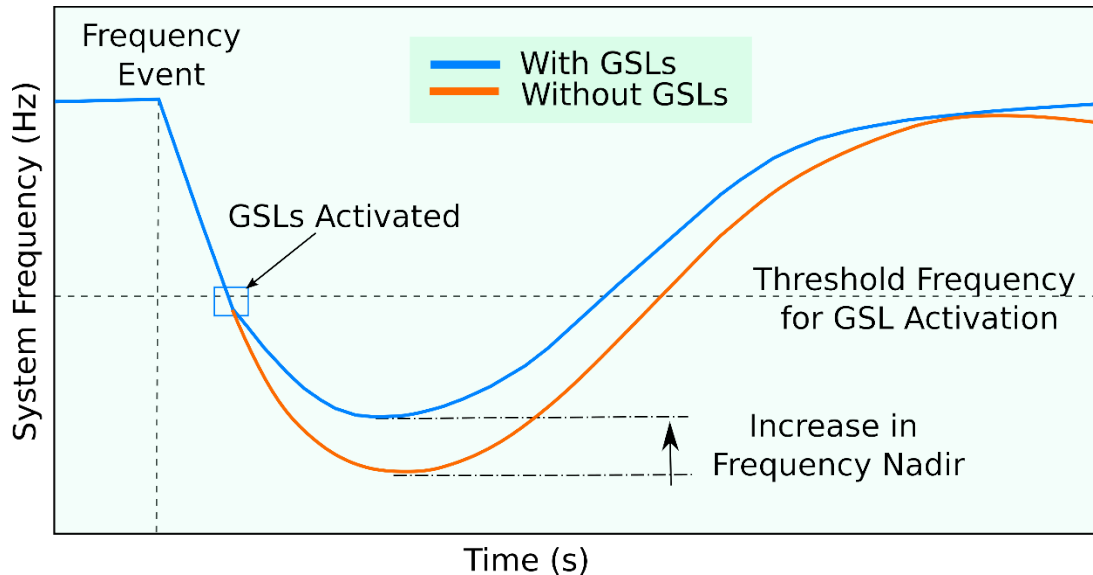


Figure 1. Impact of GSLs on frequency nadir

In addition to frequency response, grids can increase their inertia to better maintain the grid frequency. Higher inertia leads to a smaller rate of change of frequency, which allows for more time for resources to adjust their output power to counteract the shift in frequency. Technologies including synchronous condensers and clutched generators can increase system inertia (Denholm et al. 2021); however, there are costs associated with the installation, operation, and maintenance of these assets. GSLs and other devices that provide FFR can reduce the need for these technologies and reduce overall system costs.

2 Implementation of Grid-Supportive Load Functions

Jain et al. (2022) introduced the concept and model of the GSL functionality for power electronics-based loads with variable output power. The introduced GSL model consists of five major components: the voltage and frequency measurement, the frequency-power relationship, the controller delay and current limit, the load restoration, and the voltage-dependent load tripping. These components work together to adjust the output power based on the measured frequency to support the grid during a contingency event and to restore power after the event. The performance of the introduced GSL model was validated by simulation with the Western Electricity Coordinating Council 9-bus system model.

Figure 2 shows the block diagram of the hardware and firmware for the GSL functionality on the power electronics-based end-use load. The extra hardware to implement the GSL functionality comprises three major stages: the line voltage scaling, the signal isolation, and the microcontroller unit (MCU). The AC line voltage input is scaled to the signal level at the line voltage scaling stage. The scaled signal is then isolated from the AC line, as is often required to protect the circuit components and users. This isolation is also called “galvanic isolation.” The MCU then receives the scaled signal from the isolator, measures the line voltage frequency and the magnitude, and calculates the desired GSL power adjustment using the GSL model in the firmware. The output power adjustment from the GSL model is transferred to the MCU for the main load control, which is used to generate the pulse width modulation signals to operate the power electronics-based load at the main MCU controlling the end-use load. We note that many power electronics-based loads can implement GSL functions, including VFDs, DC motors, EV chargers, and other DC loads.

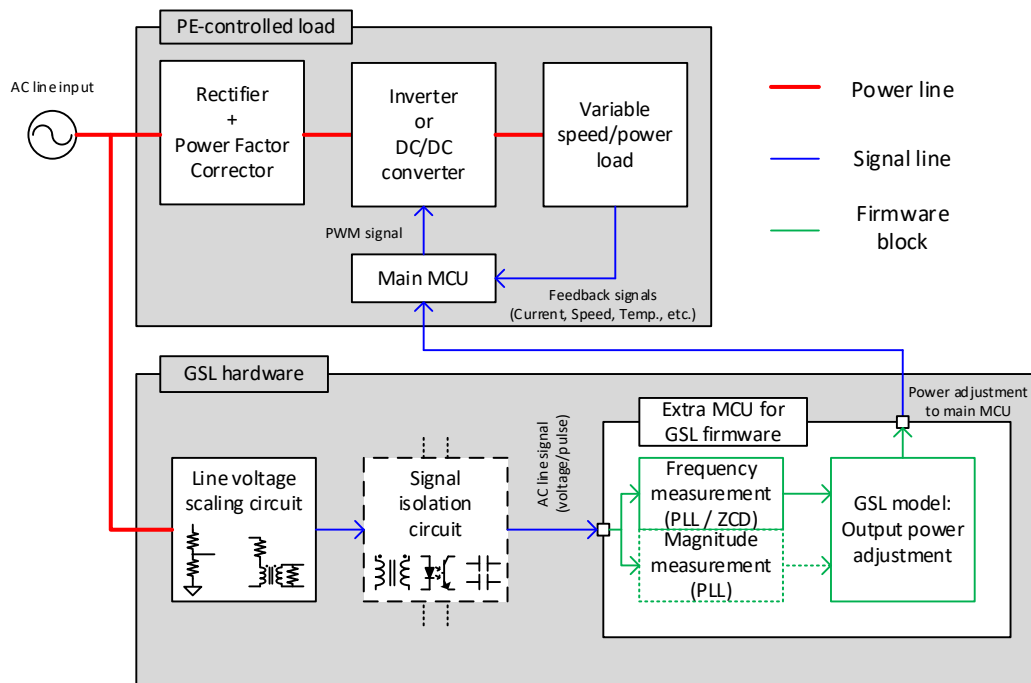


Figure 2. Block diagram of GSL hardware and firmware implementation

This report primarily focuses on the costs and impacts of frequency response in GSLs through active power adjustment. Frequency response requires only a frequency measurement, not a voltage magnitude measurement; however, GSLs can provide voltage regulation services if they can measure the voltage magnitude. Unlike most distributed generation and storage devices, most power electronics-based loads can control only their real power, not their reactive power, for voltage regulation.

2.1 Line Voltage Scaling

The main purpose of the line voltage scaling circuit is to scale the line input voltage to the signal range. Figure 3 and Figure 4 show example schematic diagrams of the line voltage scaling circuit.

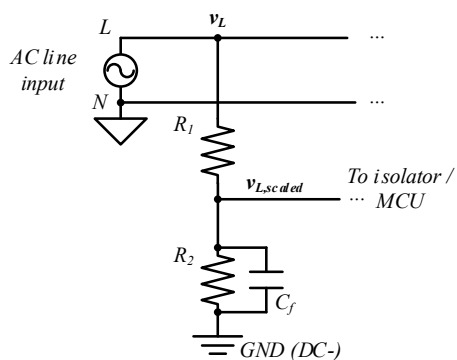


Figure 3. Line voltage scaling circuit with a voltage divider

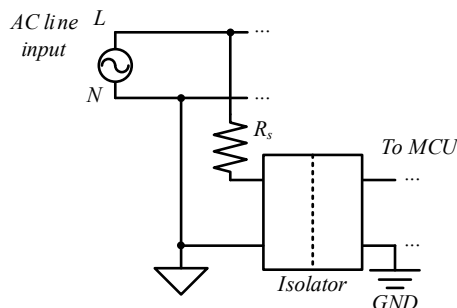


Figure 4. Line voltage scaling circuit with a shunt resistor

Figure 3 shows the resistive voltage divider, which is the most common form of implementing the voltage scaling circuit. *GND (DC-)* in the figure can be the neutral point of the voltage line or the power ground of the load circuit. The scaled voltage is calculated as:

$$v_{L,scaled} = v_L \frac{R_2}{R_1 + R_2}$$

where $v_{L,scaled}$ is the scaled line voltage, v_L is the line voltage, and R_1 and R_2 are the resistances in the voltage divider. The resistances R_1 and R_2 are designed so that the voltage across R_2 is scaled to a range that is usable for the subsequent isolation stage, or MCU. Also, the resistor R_1 is usually realized as multiple series-connected resistors because it is necessary to maintain the voltage across each individual resistor at a level less than its component rating. In the 120/240-V

AC line input load case, three 0805 size surface mount resistors (150-V rating) were usually applied at R_1 , and one 0603 size resistor (75-V rating) was applied at R_2 (Bhardwaj and Kim 2021). The total voltage rating in this case is 525 V, which is 1.5 times higher than the peak line voltage of a 240-V AC line. The current through the resistors should also be considered. The total resistance of the voltage divider is usually designed to be within the range of several megaohms to keep the current flow through the resistors within the range from tens to hundreds of microamps. This ensures negligible loss at the resistor branch. Resistors with a tolerance of less than 1% are commonly recommended for the resistor branch design.

In the voltage divider, the filter capacitor, C_f , can be placed in parallel with R_2 for noise reduction. The voltage divider with this filter capacitor will act as a first-order low-pass filter, and the bandwidth of the filter is calculated by:

$$f_{BW} = \frac{R_1 + R_2}{R_1 R_2 C_f}$$

Another way to implement the line voltage scaling circuit is to convert the line voltage into a current signal by placing the current-limiting shunt resistor, R_s , between the AC lines, as shown in Figure 4. Some current-type signal isolators—such as signal transformers, optocouplers, or voltage transducers—with hall effect sensors can be connected in series with the shunt resistor so that the scaled current signal is converted again to the analog or digital voltage signal. The resistance R_s depends on the current rating of the signal isolators. It is usually within the range of milliamps in transformers and optocouplers and within the range of tens to hundreds of microamps for capacitive digital isolators. Like voltage dividers, shunt resistors should be designed as series-connected resistors considering the voltage rating.

2.2 Signal Isolation

Galvanic isolation prevents unwanted current flow between electrical systems with different grounds. The main reason for the isolation is to protect operators and electrical devices from severe damage while transferring power and/or a voltage or current signal. For safety reasons, most appliances implement galvanic isolation between power conversion circuits and the human-machine interface (Bonifield 2017). Also, in some high-power applications, an isolated power conversion circuit is applied to protect power switches and controllers from severe damage (Kamath 2015).

For GSL hardware, a signal isolation circuit will be required between the line voltage scaling circuit and the controller circuit when these two circuits are placed on different electrical grounds. Optocouplers, transformers, and capacitive digital isolators are the most widely used circuits for signal isolation.

The optocoupler circuit is a common cost-effective way to implement a digital signal isolator. It uses a light-emitting diode (LED) to convert the input current into an isolated optical signal, and it uses an accompanying phototransistor to detect it. Because of its cost-effectiveness, the optocoupler is widely used as a digital isolator, especially for cost-sensitive applications; however, it has performance and reliability difficulties related to the characteristics of the LED—it requires relatively high current (typically up to 25 mA) to turn on the LED and has low

bandwidth due to its long propagation delay (Kliger 2003). The need for relatively high current should be considered in the GSL hardware design because high current through the optocoupler can reduce the efficiency and reliability of the end-use hardware. The resistance of the current-limiting shunt resistor should be large enough to reduce the energy losses and small enough to ensure the reliability of the optocoupler operation. Additional components (e.g., comparators, operational amplifiers, voltage-controlled oscillators) can also be placed between the optocoupler and the line voltage scaling circuit to mitigate this issue.

The transformer circuit is one of the most common ways to transfer both power and a signal through an isolated barrier. It can directly couple the AC signals through magnetic coupling. It does not require auxiliary circuits at the primary side, but the transformer itself can be a barrier to making the circuit small and cost-effective. In particular, the line frequency transformer is much larger and heavier than a transformer for higher frequency. To mitigate the size and weight issue, some line frequency transformers with current ratings up to several milliamps, called current-type microminiature voltage transformers, are designed to measure the line frequency voltage for grid applications (Yao et al. 2020).

The capacitive digital isolator circuit isolates the signal using capacitive coupling with silicon-dioxide as a dielectric. It features high-speed, low-power signal transmission performance, and it has low susceptibility to electromagnetic noise. It is becoming more common as the price of the isolator decreases, but it is still more expensive than the optocoupler. It is also easier to combine other circuits into a single integrated circuit chip. Most isolated operational amplifiers consist of analog-to-digital converters (ADCs), digital isolators, and digital-to-analog converters. These devices convert the analog signal into a digital signal, send the digital signal to the secondary (controller) side, and reconvert the digital signal into an analog signal for output (Maniar 2019).

2.3 Frequency Detection

The scaled and isolated line voltage signal is then used to calculate the grid frequency. There are two major methods to measure the line frequency from the AC signal: phase-locked loop (PLL) and zero-crossing detection (ZCD).

The PLL method is widely used in grid-connected inverters to measure the frequency, the phase, and the amplitude of the line voltage, which are used to synchronize the output voltage of the inverter to the line voltage and to control the output power of the inverter. There are several forms of PLL for line frequency measurement. A commonly used PLL structure for a three-phase system uses a synchronous reference frame (Rodriguez et al. 2007), which is shown in Figure 5. The voltage vector is transformed into a dq synchronous reference frame, and the phase angle of the dq reference frame is generated from the v_q controller. By using this structure, the voltage magnitude, v_d , and the frequency/phase of the voltage vector can be obtained in the steady state. Based on this structure, many other forms of PLLs are introduced to enhance the bandwidth, reduce the noise, or reduce the computational time. The same PLL structure used for three-phase systems can be applied to single-phase systems by generating the quadrature component of the original AC signal (Subedi et al. 2022). These PLL structures for grid-connected inverters can also be used to implement the frequency measurement part of the GSL model. The settling time of the PLL block depends on the controller gain, and the practical gain design allows the PLL to settle within a single cycle for a three-phase PLL or within two cycles for a single-phase PLL (Kulkarni and John 2013).

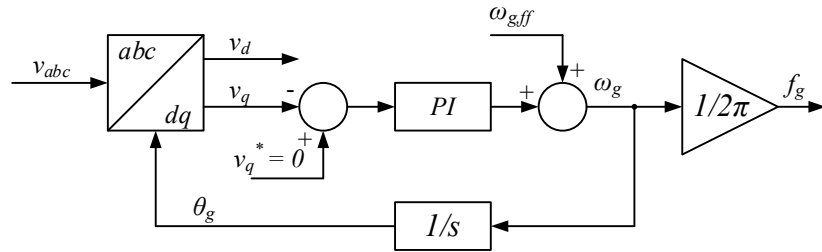


Figure 5. PLL block diagram for three-phase line-connected load

Source: Based on the model from Rodriguez et al. 2007

The ZCD method is a widely used method in the industry. Figure 6 shows conceptual diagrams of the ZCD method. This method generates the pulse at the zero crossing of the input signal and calculates the frequency by measuring the time between pulses or by counting the pulses within a certain time period. Because it typically has a lower computational burden than the PLL method and it does not require an ADC channel on the MCU or other integrated circuit chips, it is widely applied across applications, including power factor correction controllers and energy metering integrated circuits; however, it can generate false zero-crossing pulses due to noise in the input signal, which can lead to frequency calculation errors, and therefore filtering the AC/pulse input signal and using the hysteresis technique is required to reduce the error to within an accepted boundary. In practical use, the ZCD method can detect the frequency within a single cycle with approximately 4 ms of blanking time to avoid false triggers (Sahasrabudhe 2019).

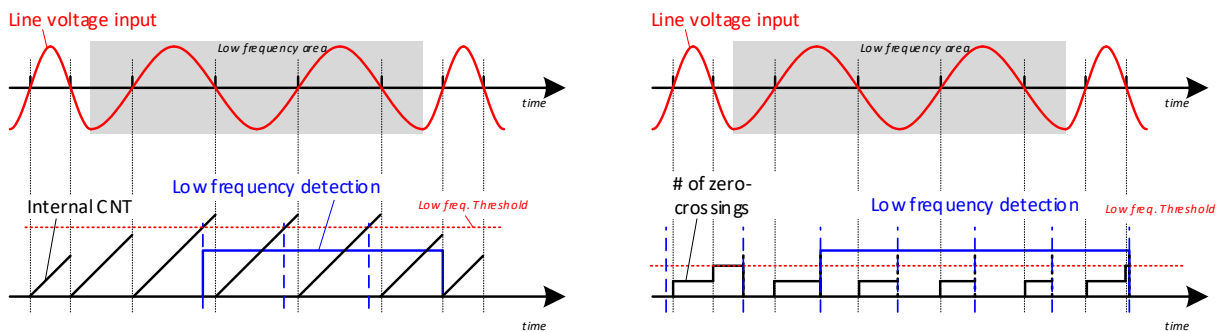


Figure 6. Conceptual diagrams of the ZCD method using the time between pulses (left) and the number of zero crossings between the fixed time period (right)

2.4 Grid-Supportive Load Control Implementation

The GSL firmware control implementation uses the line frequency measurement and sends an output power adjustment signal to the main MCU. The output power adjustment can be implemented in many different forms, depending on the type of load. One simple option is to turn the device off at a given low-frequency threshold; however, this control can cause voltage and frequency stability issues if many GSLs are turned on or off at the same time, and it can lead to device degradation by quickly cycling the device on and off.

One likely control implementation is a frequency-watt droop curve, as shown in Figure 7. These curves are used in the Institute of Electrical and Electronics Engineers' (IEEE) Std 1547 for defining the frequency response characteristics of distributed generation and storage devices

(IEEE 2018). The curve is characterized by the threshold frequency of activation, the droop slope, and a minimum power limit (Hoke et al. 2017). These parameters will impact the amount of frequency response provided by the device.

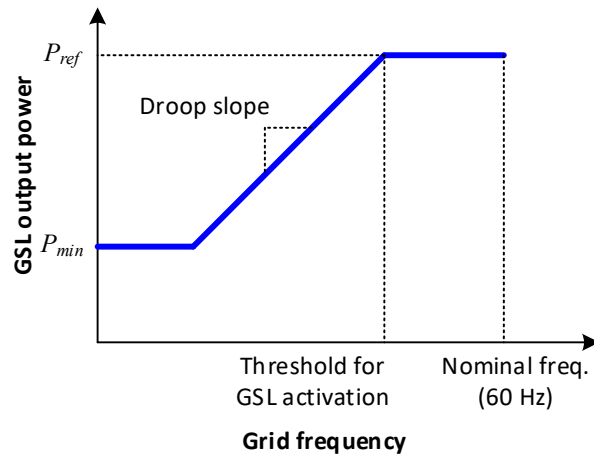


Figure 7. Frequency-watt curve for GSL control implementation

The GSL model firmware can be implemented on either a GSL-dedicated MCU or the main MCU. If there is an available input pin, an ADC channel, and enough computational time and memory for running the GSL function code, the GSL model can be implemented in the existing main load controller MCU. If these resources are not available, however, an extra GSL-dedicated MCU can be included to implement the GSL model. Low-cost MCUs can be used because the GSL model firmware does not require a significant amount of computational time or memory.

2.5 Grid-Supportive Load Hardware Design Classification

GSL hardware implementation can be classified into five designs based on the line voltage scaling circuit, the signal isolation circuit, and the type of signal interfaced with the MCU. The detailed component design and bill of materials (BOM) for each design is explained in Section 3.1. Note that either frequency detection method can be used for each circuit design.

The Type I design, shown in Figure 8, is for non-isolated systems in which the system has the connected ground between the main load controller and the connected power stage. Because signal isolation is not used in this design, cost-effective GSL hardware can be configured with only a voltage divider and the MCU.

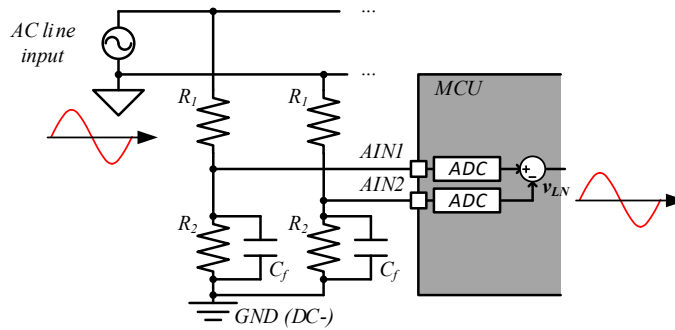


Figure 8. Type I design: non-isolated design with voltage divider

The Type II design, shown in Figure 9, uses a voltage divider as a line voltage scaling circuit and sends the analog signal to the MCU. In this case, an isolated operational amplifier is typically used for isolation. This is because it has the advantage of accurately transmitting a scaled voltage signal due to the performance of the capacitive isolator. The cost of the isolated amplifier itself is significant, however, and it requires some additional circuits to supply power to the amplifier.

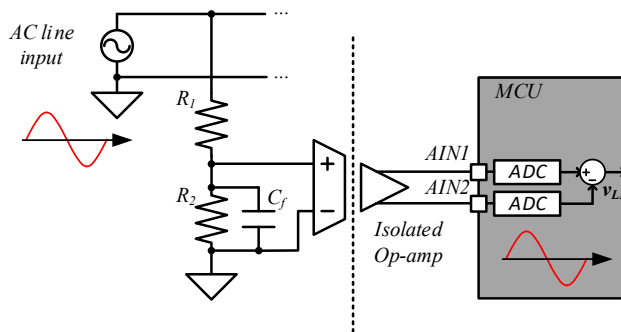


Figure 9. Type II design: isolated design with voltage divider and analog output

The Type III design, shown in Figure 10, applies the voltage divider with a digital signal isolator. Sending a digital signal to the MCU has the advantage of applying a cost-effective isolator, such as an optocoupler, and does not require a reserved ADC channel on the MCU; however, this circuit has limited line voltage magnitude measurement feature that can only detect whether the voltage is over a given threshold. Therefore, this design can be appropriate for frequency-responsive GSL implementation but not for voltage-responsive GSL capabilities.

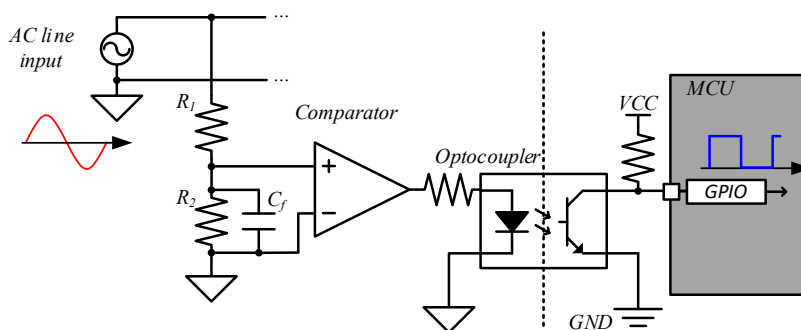


Figure 10. Type III design: isolated design with voltage divider and digital output

The Type IV design, shown in Figure 11, uses a current-limiting shunt resistor and transmits an analog signal to the MCU. In this case, a current-type transformer or a hall sensor-based voltage transducer can be used as an isolator. The advantage of this design is that it does not require additional components other than resistors and the isolator on the primary (i.e., line voltage) side; however, the transformer has disadvantages in terms of its weight and volume, and the voltage transducer is relatively expensive. Recently, a small current-type line frequency voltage transformer for line voltage sensing was introduced that mitigates the weight and volume disadvantages of the line frequency transformer (Yao et al. 2020).

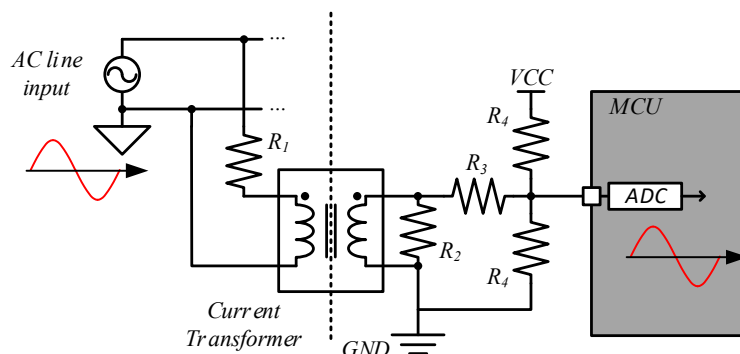


Figure 11. Type IV design: isolated design with current-limiting resistor and analog output

Figure 12 shows the Type V design with the current-limiting resistor and the digital signal output. This design is widely used in low-voltage digital signal receivers because of its simple structure and low-cost components. If this circuit design is applied to the AC power input of 120/240 V instead of typical low-voltage circuits, the power loss in the resistor can be significant. Replacing the optocoupler with a capacitive digital isolator can mitigate this problem because it has a much lower input current rating. The Type V design can also include isolated signal receivers that do not require a separate power source for the primary side, which can reduce the cost.

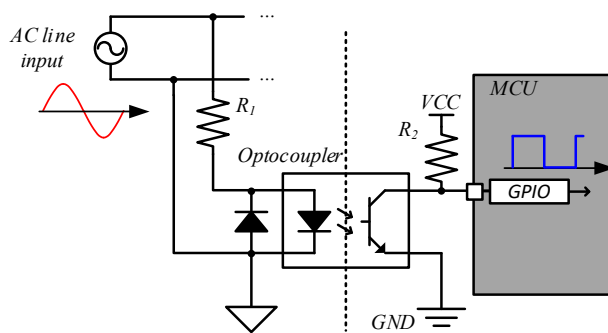


Figure 12. Type V design: isolated design with current-limiting resistor and digital output

Additional operational amplifiers or comparators can be used to more accurately scale the line voltage signal or to generate pulse data from the analog grid voltage signal. If additional circuits are placed at the line voltage sensing side, an additional isolated DC-DC converter or bootstrap circuit would be required to supply power to the additional active components.

3 Grid-Supportive Load Implementation Costs

In this section, we estimate the cost of the extra circuitry for the GSL hardware implementation for multiple types of end-use loads. GSL functions can be applied to various types of power electronics-based loads, such as equipment with a VFD (e.g., heat pumps, heat pump water heaters, refrigerators, other home appliances) and DC loads with an AC/DC converter (e.g., EV chargers, LED lighting, DC motors). The effect of GSLs on the grid depends on several factors, including the total energy consumption, the load profile, and the control flexibility (Blonsky, Subedi, and Mather 2022). Refrigerators, EV chargers, and HVAC are expected to have large potential benefits as GSLs. Refrigerators have relatively high energy consumption levels and a nearly constant load profile regardless of the season due to their operation in conditioned space. EVs and EV chargers are expected to have high energy consumption levels, and they have a high degree of short-term flexibility. Heat pumps for HVAC also have high energy consumption levels and are expected to see rapid deployment in the future. These end uses were selected as the target load types to analyze the cost of extra circuitry. While this report focuses on residential loads, GSLs can be applied to power electronics-based commercial loads as well.

For all these load types, we selected GSL components, and we evaluated the implementation costs for multiple hardware designs. Based on the cost evaluation results, we present the most cost-effective design for the target application. Single-phase, 120-V AC voltage is assumed as the input voltage for the residential refrigerator. Single-phase, 240-V AC voltage is assumed for Level 2 EV chargers and residential HVAC equipment. Three-phase 208-V AC voltage is assumed for Level 3 EV chargers (i.e., DC fast chargers). In this report, galvanic isolation is assumed for all applications, although it might not be required for small appliances.

This report does not consider other capital or operational costs associated with GSL implementation. Other capital costs could include the design, testing, and assembly required for adding GSL hardware and modifying existing hardware. Operational costs could include measurement and verification and any negative effects on the end-use service or the device lifetime.

3.1 Hardware Costs

Hardware costs are estimated for each of the five designs described in Section 2.. The component cost values are from component manufacturers in June 2022, based on a unit price of 1,000 units. The costs are reported for single-phase and three-phase circuits. The scope of the cost estimate is limited to the price for components only. Costs for other items—such as circuit board design, fabrication, and assembly costs; testing and debugging costs; and other labor costs—are excluded in this estimation.

We assume that the device will need an extra MCU to handle the additional calculations required for GSL functionality. The extra MCU circuit includes the MCU chip with bypass capacitors and some resistors. Table 2 shows the list of cost-effective MCUs with an internal ADC block, which can be used for the GSL implementation. MSP430G2152IRA16R is selected from the MCUs in the table due to its low cost and high performance.

Table 2. Cost-Effective MCUs With Internal ADC Block

Model	Unit Price	Note
MSP430G2152IRSA16R	\$0.78	MSP430 core, 16 bit, 16 MHz, 10 bit ADC
ATTINY40-SU	\$0.51	AVR core, 8 bit, 12 MHz, 10 bit ADC
PIC16F15223-I/MG	\$0.59	PIC core, 8 bit, 32 MHz, 10 bit ADC
MS51DA9AE	\$0.44	8051 core, 8 bit, 24 MHz, 12 bit ADC
XMC1201T028F0032ABXUMA1	\$1.07	Cortex-M0+ core, 32 bit, 40 MHz, 12 bit ADC

The Type I design consists of line voltage scaling circuit branches and an extra MCU for firmware implementation. For the line voltage scaling circuits, two branches are required in the single-phase voltage input cases, and three branches are required in the three-phase input cases. In each voltage divider branch, R_2 is usually implemented with a single surface mount resistor, and the size and number of resistors at the upper resistance, R_1 , are determined by the voltage rating of the surface mount resistor and the current through the branch. We choose a tolerance of at least 1% for the resistors. The filter capacitor at each branch is usually designed with a single surface mount capacitor. The reference AC/DC converter design (Bhardwaj and Kim 2021) uses three 0805 size resistors for R_1 , one 0603 size resistor for R_2 , and one 0603 size capacitor for the filter capacitor.

Table 3 shows the BOM for the Type I design with a single-phase input. The Type I design costs approximately \$0.92 for single-phase systems, \$0.41 for the line voltage sensing circuit, and \$0.51 for the extra MCU circuit. In the three-phase cases, the design costs approximately \$1.12 because the line voltage sensing circuit costs approximately \$0.62.

Table 3. BOM and Cost Estimates for Single-Phase Type I Design

Circuit	Part	Value	Quantity	Unit Price	Subtotal
Stage I: Line voltage scaling circuit	Scaling R (R_1)	402 kOhm/0.1%	6	\$0.0506	\$0.4126
	Scaling R (R_2)	10 kOhm/0.1%	2	\$0.0506	
	Filtering C	10 nF/50 V/X7R	2	\$0.0041	
	MCU	MSP430G2152IPW14R	1	\$0.4660	
Stage III: Extra MCU	Decoupling C	10 uF/10 V/X7R	1	\$0.0322	\$0.5058
	Decoupling C	100 nF/10 V/X7R	1	\$0.0057	
	Pull-up R at /RST pin	47 kOhm/1%	1	\$0.0019	
Total					\$0.9183

The Type II design requires one resistor branch for the line scaling circuit, an isolated amplifier, and an extra MCU. The same aspects as explained in the Type I design case are considered during the component selection for the line voltage scaling circuit and the extra MCU circuit. AMC1000DWVR from Texas Instruments is selected for the isolated amplifier for the voltage/current sensing. An additional DC-DC converter circuit is included to supply the primary side of the isolated amplifier.

Table 4 shows the BOM and cost estimates of the Type II design connected to a single-phase line. As shown, the cost for the isolated amplifier and an additional circuit is approximately \$3.48, which is a significant amount of the total cost. For the three-phase line input load, the total cost increases to \$11.84 because the isolated amplifier circuit needs to be separately configured for each phase.

Table 4. BOM and Cost Estimates for Single-Phase Type II Design

Circuit	Part	Value	Quantity	Unit Price	Subtotal
Stage I: Line voltage scaling circuit	Scaling R (R ₁)	1 MOhm/0.1%	4	\$0.0638	
	Scaling R (R ₂)	2 kOhm/0.1%	1	\$0.0411	\$0.2993
	Filtering C	10 nF/ 50 V/X7R	1	\$0.0031	
Stage II: Signal isolation circuit	Isolation op-amp	AMC1100DWVR	1	\$1.8420	
	Filtering C	10 nF/50 V/X7R	1	\$0.0031	
	Decoupling C	100 nF/10 V/X7R	2	\$0.0304	\$3.4782
	DC/DC converter	PDSE1-S5-S5-S	1	\$1.5400	
	Decoupling C	1 uF/10 V/X7R	2	\$0.0162	
Stage III: Extra MCU	MCU	MSP430G2152IPW14R	1	\$0.4660	
	Decoupling C	10 uF/10 V/X7R	1	\$0.0322	
	Decoupling C	100 nF/10 V/X7R	1	\$0.0057	\$0.5058
	Pull-up R at /RST pin	47 kOhm/1%	1	\$0.0019	
Total					\$4.2833

The Type III design applies the optocoupler and comparator to convert the line voltage input into a digital pulse signal and transmit it to the MCU. Like the Type II design case, an additional DC-DC converter circuit is required to supply the comparator. Table 5 shows the BOM and cost estimates of the single-phase line input Type III design. By applying the optocoupler, the cost of the signal isolation stage can be reduced to approximately \$2.00. In the three-phase line input cases, the overall cost increases to approximately \$7.10 because the line voltage scaling and the signal isolation stages need to be configured at each phase.

Table 5. BOM and Cost Estimates for Single-Phase Type III Design

Circuit	Part	Value	Quantity	Unit Price	Subtotal
Stage I: Line voltage scaling circuit	Scaling R (R ₁)	402 kOhm/0.1%	3	\$0.0506	
	Scaling R (R ₂)	10 kOhm/0.1%	1	\$0.0506	\$0.2063
	Filtering C	10 nF/50 V/X7R	1	\$0.0041	
Stage II: Signal isolation circuit	Comparator	LM339DT	1	\$0.1677	
	Optocoupler	HCPL-817-50BE	1	\$0.1778	
	Resistor	190 Ohm/1%	1	\$0.0067	
	Pull-up resistor	1 kOhm/1%	1	\$0.0107	
	Filtering C	10 nF/50 V/X7R	1	\$0.0031	\$1.9991
	Decoupling C	100 nF/10 V/X7R	2	\$0.0304	
	Isolated DC/DC converter	PDSE1-S5-S5-S	1	\$1.5400	
	Decoupling C	1 uF/10 V/X7R	2	\$0.0162	
Stage III: Extra MCU	MCU	MSP430G2152IPW14R	1	\$0.4660	
	Decoupling C	10 uF/10 V/X7R	1	\$0.0322	\$0.5058
	Decoupling C	100 nF/10 V/X7R	1	\$0.0057	
	Pull-up R at /RST pin	47 kOhm/1%	1	\$0.0019	
Total					\$2.7111

The Type IV and Type V designs apply current-limiting shunt resistors at the line voltage scaling stage instead of the voltage divider. The resistance of the shunt resistors is determined by considering the current rating of the signal isolator. Also, like the R_I component selection in the voltage divider design, the number and size of the resistors depend on the line voltage and the maximum voltage of the resistor chip. For the Type IV design, a 2-mA current-type voltage transformer is selected. This requires a shunt resistance of approximately 240 kOhm, which can limit the steady-state current to less than 1 mA for a 240-V line input. For the Type V design, the optocoupler can be applied for the signal isolation, and the resistance of the shunt resistor depends on the LED turn-on current of the optocoupler. In this evaluation, the shunt resistor is designed as 120 kOhm, which can turn on the optocoupler LED at an input voltage of 120 V.

Table 6 and Table 7 show the BOM and cost estimates of the Type IV and Type V designs connected to a single-phase line, respectively. Type IV and Type V are the most cost-effective designs for isolated systems with analog signal outputs and digital signal outputs, respectively. This is because they do not require additional circuits and a DC-DC converter to supply power at the primary side of the isolator, which reduces the implementation cost for the signal isolation stage to \$1.76 for Type IV and \$0.43 for Type V. In three-phase line input cases, the total implementation cost increases to \$6.12 for Type IV and \$2.46 for Type V.

Table 6. BOM and Cost Estimates for Single-Phase Type IV Design

Circuit	Part	Value	Quantity	Unit Price	Subtotal
Stage I: Line voltage scaling circuit	Shunt R (R ₁)	475 kOhm/1%/0.25 W	2	\$0.0550	\$0.1100
	Burden R (R ₂)	400 Ohm/0.1%	1	\$0.0489	
Stage II: Signal isolation circuit	Scaling R (R ₃)	10 kOhm/0.1%	1	\$0.0472	\$1.7605
	Scaling R (R ₄)	100 kOhm/0.1%	2	\$0.0472	
	Current transformer	YHDC—TV16	1	\$1.5700	
Stage III: Extra MCU	MCU	MSP430G2152IPW14R	1	\$0.4660	
	Decoupling C	10 uF/10 V/X7R	1	\$0.0322	\$0.5058
	Decoupling C	100 nF/10 V/X7R	1	\$0.0057	
	Pull-up R at /RST pin	47 kOhm/1%	1	\$0.0019	
Total					\$2.3763

Table 7. BOM and Cost Estimates for Single-Phase Type V Design

Circuit	Part	Value	Quantity	Unit Price	Subtotal
Stage I: Line voltage scaling circuit	Shunt R (R ₁)	475 kOhm/1%/0.25W	4	\$0.0550	\$0.2200
	Pull-up R (R ₂)	1 kOhm/1%	1	\$0.0107	
Stage II: Signal isolation circuit	Optocoupler	140354245000	1	\$0.3900	\$0.4311
	Decoupling C	100 nF/10 V/X7R	1	\$0.0304	
	MCU	MSP430G2152IPW14R	1	\$0.4660	
Stage III: Extra MCU	Decoupling C	10 uF/10 V/X7R	1	\$0.0322	\$0.5058
	Decoupling C	100 nF/10 V/X7R	1	\$0.0057	
	Pull-up R at /RST pin	47 kOhm/1%	1	\$0.0019	
Total					\$1.1568

Table 8 shows the summary of the cost estimates of the GSL hardware designs. The Type I and Type V designs are the most cost-effective designs for non-isolated systems and isolated systems, respectively. If the analog signal output is required to measure the input voltage amplitude, then the Type IV design can be a good alternative for isolated systems.

Table 8. Summary of the Cost Estimates for the Five Hardware Designs

Design Type	Cost (Single Phase)	Cost (Three Phase)	Signal Type (to MCU)	Note
Type I	\$0.93	\$1.12	Analog	Cost-effective design for non-isolated systems
Type II	\$4.28	\$11.84	Analog	Design for accurate voltage measurements in isolated systems
Type III	\$2.71	\$7.10	Digital	Alternative design for isolated systems with digital signal output
Type IV	\$2.37	\$6.12	Analog	Cost-effective design for isolated systems with analog signal output
Type V	\$1.15	\$2.46	Digital	Cost-effective design for isolated systems

We note that the additional energy consumed by the GSL hardware is very low compared to the energy consumption of the device. For example, consider the energy consumed by the sensing circuit in the Type V design, shown in Figure 12, where $R_l = 120 \text{ k}\Omega$, and the input line voltage is single-phase 120 V. The conduction loss at the current-limiting resistor, R_l , dominates the total loss from the sensing circuit. Assuming that there is no forward voltage drop at the optocoupler LED, the root mean square current flowing through the resistor R_l is 1 mA, and the power loss from R_l is $(1 \text{ mA})^2 (120 \text{ k}\Omega) = 0.12 \text{ W}$. Similar standby losses are expected from the other designs. If the sensing circuit is always on, the annual energy loss from the sensing circuit is 1.05 kWh/year. Assuming a \$0.10/kWh cost of electricity and a 10-year lifetime, this amounts to a cost of approximately \$1 over the life of the device. Using an average annual energy consumption of 362 kWh/year for a residential refrigerator (see Section 5.3), the added GSL hardware would increase the annual energy consumption by 0.29%. This increase would be smaller for other devices that have higher annual energy consumption levels, e.g., EVs and HVAC systems. It is also possible that the sensing circuit can be integrated with existing hardware to minimize energy losses.

3.2 Cost-Effective Designs for End-Use Equipment

Figure 13 shows a commonly used topology for residential refrigerators. Although it is not shown, we assume that the refrigerator requires isolation for the digital signal controller. Given the need for signal isolation and a digital signal type, the Type V design is the most cost-effective solution for this system. The estimated implementation cost for the GSL hardware is \$1.15 for this case. The cost can be further reduced if a voltage divider already exists for power factor correction control and protection and can be used by the GSL. The costs for the extra MCU can also be removed if there are available ADC channels at the main load controller MCU.

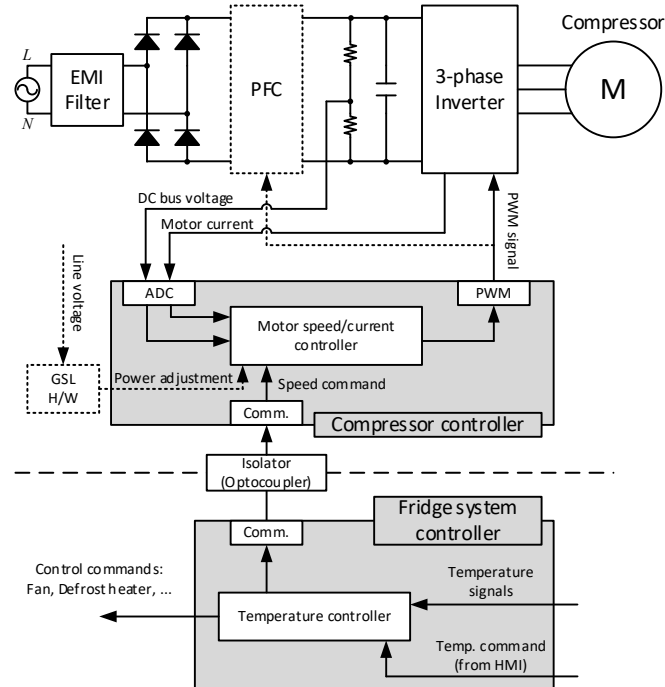


Figure 13. Common topology of a power electronics-based residential refrigerator with optional GSL hardware

Source: Derived from NXP Semiconductors 2022

In contrast, a three-phase Level 3 EV charger usually isolates the AC/DC power conversion stage, the DC/DC power conversion stage, and the controller stage, as shown in Figure 14. This is because its high voltage and power levels require higher safety standards. Type V or Type IV are the cost-effective designs that can be applied in this isolated system, and the implementation cost would be \$2.46 for Type V and \$6.12 for Type IV.

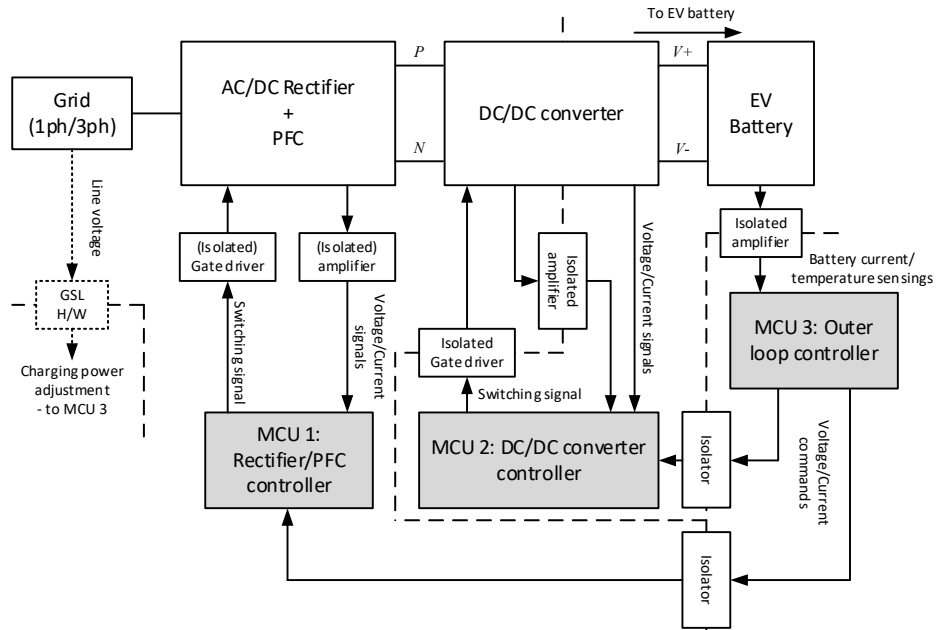


Figure 14. Common topology of an EV charger with optional GSL hardware

Source: Derived from Gong and Rangaraju 2018

Level 2 EV chargers and large residential HVAC systems run on single-phase 240 V and often require isolation. Based on these requirements and the costs presented in Table 8, the Type IV or Type V hardware designs would be the most cost-effective solutions. The Type V design would cost \$1.15, and the Type IV design would cost \$2.37.

4 Market Impacts of Grid-Supportive Loads

GSL adoption at scale will impact the existing methods for procuring frequency response and other grid services. In this section, we consider mechanisms that might be required to incentivize GSL adoption, and we estimate the quantity of frequency response that can be procured with GSLs.

4.1 Grid-Supportive Load Adoption Pathways

GSLs provide benefits to grid operators by providing frequency response and other ancillary services. The costs of GSLs are incurred by the device manufacturer in the form of extra hardware, integration, testing, and verification. These costs are likely to be passed to the consumer; however, grid operators might not be willing to compensate consumers for their GSL benefits for multiple reasons:

1. Grid operators might not be aware that GSLs are active and functioning because GSLs are autonomously controlled and have limited communication requirements.
2. The benefits are diluted across many devices (on the order of \$1 per device per year), which makes direct, individual procurement an expensive option.
3. GSLs only provide low-frequency response when they are consuming power, and power consumption often depends on consumer behavior, which can lead to uncertainty in the quantity and timing of the benefits.

The first issue can be addressed by developing a certification and/or standard for GSL implementation with requirements for the level of service provided. A certification can require evaluation, measurement, and verification to provide grid operators with more confidence that the GSL is providing the desired services. It can also serve as a marketing tool for manufacturers to highlight the capabilities of their products.

A standard could limit the ability for manufacturers and consumers to disable or adjust the GSL functionality. It could also standardize communication and control protocols and specifications. The standard could be based on IEEE Std 1547, which is designed for distributed energy resources (DERs) with generation capabilities and includes specifications for frequency response (IEEE 2018). The GSL standard would differ from IEEE Std 1547 because it would apply only to energy-consuming devices.

To address the remaining issues, there must be a mechanism that allows manufacturers or consumers to monetize the value that GSLs provide. There are many policies and market mechanisms that are used for similar products that could apply to GSLs. Note that all the mechanisms might require state or federal regulatory approval and oversight.

One-time incentive or rebate: A one-time incentive or rebate could be applied to the purchase or installation of a product with GSL functionality to offset the additional cost of implementation. Similar to incentives and rebates for energy-efficient equipment, this mechanism could be applied to the manufacturer, to the contractor or installer, or directly to the consumer. Incentives could be provided by the local utility or grid operator. Although this mechanism is simple to implement, it does not allow the utility or grid operator to adjust the compensation amount based on observed grid benefits, which can depend on geography, season, and occupant behavior.

Recurring incentive program: Utilities or DER aggregators could create demand-side management programs that compensate participants for the use of their GSL on a recurring basis, e.g., monthly or annually. The program could include device registration, measurement and verification, or communication requirements to ensure that GSLs are providing the expected amount of frequency response. This mechanism would enable more flexibility and control than a one-time incentive; however, programs would need to be cost-effectively designed to ensure that program costs do not exceed the GSL benefits on a per-device basis.

Independent system operator market product: A frequency response (or, more broadly, ancillary service) market would enable more precise control over the compensation to GSLs. The market would vary the price of the service over time. It could also include penalties to ensure that GSLs are providing the required service, though this would require measurement and verification with each device that could be expensive to implement. This information can be communicated after the frequency event occurs such that it does not delay the frequency response. Because the value of a single GSL is very small, aggregators would be essential to bundle GSLs together to bid into the market. Similar to aggregators for DER energy and flexibility services, these aggregators would be responsible for communicating with individual devices, ensuring that they are active, managing uncertainty in their use, and compensating consumers for their participation.

Product requirement: The simplest mechanism for encouraging GSL adoption is to require GSL functionality for certain product types within a given jurisdiction. Rather than compensating consumers for the value of GSLs, it would require all products sold or installed to include GSL functionality. This would likely increase the cost of the product and reduce the cost of grid operations, which could get passed to consumers through lower electricity rates. Product requirements are effectively used for similar use cases, including in energy-efficient equipment standards, in building codes, and in California Rule 21, which effectively requires DERs with inverters to provide frequency response and voltage regulation services (California Public Utilities Commission 2017).

4.2 Meeting Frequency Response Requirements

Given the relatively small energy consumption level of a single load, many GSLs will be necessary to provide enough frequency response to cause a substantial change in grid frequency. We calculate the number of GSLs required to provide all frequency response that is currently required in the United States. This analysis assumes that all GSLs can be fully shut off during a low-frequency event and that load profiles are constant.

The North American Electric Reliability Corporation recommends an Interconnection Frequency Response Obligation (IFRO) for regions with multiple grids. The IFRO is defined as the amount of generation growth that must take place per unit of frequency decline (MW/Hz). The product of the IFRO and the maximum delta frequency is the frequency response requirement (FRR). The FRRs for the three interconnections in the contiguous United States are 1,543 MW for the Electric Reliability Council of Texas (ERCOT), 2,402 MW for the Western Interconnection, and 4,263 MW for the Eastern Interconnection (Jorgenson and Denholm 2019). We sum these values to create a national frequency response total requirement of 8,208 MW.

To estimate the number of GSLs needed to meet these requirements, we estimate the annual energy consumption and average power of a typical GSL. For refrigerators, the most common type is a two-door, top-freezer fridge with an average capacity of 20–22 ft³ (EIA 2020). This aligns with products in the ENERGY STAR[®] list of refrigerators with “advanced adaptive compressors” (ENERGY STAR 2021). These products use VFDs and generally have higher efficiency than all other refrigerators. The average annual energy consumption for a refrigerator in these categories is 362 kWh/year, which corresponds to an average power of 44.5 W.

We also estimate the potential number of available GSL devices by end use in ERCOT and across the United States. We assume that the number of available refrigerators is equal to the number of refrigerators currently in use and that all refrigerators will have VFDs or are otherwise capable of providing GSL services. The number of available refrigerators in Texas (to compare to the ERCOT interconnection) is taken from the National Renewable Energy Laboratory’s (NREL’s) End-Use Load Profiles project (Present 2019), and the number of available refrigerators across the United States is taken from the EIA (2020).

For EV chargers, the annual energy consumption depends on the location of the charger (home, workplace, etc.) and the charger level. We use the projected annual energy consumption and number of chargers from a recent NREL report (Wood et al. 2023). Combining all types of Level 2 chargers, the report estimates an annual energy consumption of 11.15 GWh in 2030 across 18.5 million chargers, which corresponds to an average power of 602 W/device. For Level 3 chargers in 2030, the annual energy consumption is projected to be 2.2 GWh from 152,000 chargers, or an average power of 14.52 kW/device. The report also projects these values by state, and the projected values for Texas (to compare to the ERCOT interconnection) are 623 W for Level 2 chargers and 16.01 kW for Level 3 chargers. The report estimates that Level 3 chargers consume 24 times more power than Level 2 chargers.

For HVAC, annual energy consumption significantly varies based on climate and the type of equipment installed. We use NREL’s End-Use Saving Shapes to estimate the energy consumption of a typical HVAC system in the United States in 2030 (Present et al. 2022).² We estimate the average annual energy consumption for a heat pump to be 5,439 kWh, which corresponds to the estimated average power of 621 W. For ERCOT, the average annual energy consumption is 4,077 kWh, which corresponds to 465 W. HVAC energy consumption in ERCOT is less than the national average because Texas has a warm climate, and colder climates are more likely to have higher HVAC consumption. Due to a lack of forecasting for heat pumps, we report the actual number of heat pumps from 2020 (EIA 2020), and we note that heat pump installation is likely to increase in the next decade (Mai et al. 2018).

Table 9 compares the potential number of available devices and the number of required GSLs to meet current FRRs for ERCOT and across the United States. In general, these devices can

² The End-Use Saving Shapes are load profiles that represent the U.S. building stock with various energy-efficiency and electrification upgrades. We use the “Heat pumps, high-efficiency, electric backup” package, which assumes that every home in the United States has a high-efficiency heat pump, to estimate the average annual energy consumption for a heat pump in 2030.

provide a substantial amount of the FRR, though it often requires millions of devices to be equipped with GSL capabilities.

Table 9. Number of GSL Devices Available and Required to Meet Current FRRs for ERCOT and Across the United States

GSL Device	ERCOT			United States		
	Available Units	Required Units	% of Required FRR	Available Units	Required Units	% of Required FRR
Refrigerator	9.3 M	34.67 M	27%	123 M	184.45 M	67%
Level 2	1.36 M	2.47 M	55%	18.5 M	13.64 M	136%
Level 3	12049	96341	13%	151869	565173	27%
HVAC Heat Pump	2.16 M ^a	3.3 M	65%	17.75 M ^a	13.2 M	134%

^a Due to a lack of forecasting for heat pumps, we report the actual number of units installed in 2020 instead of the estimated number of units available in the future.

The total hardware cost of providing frequency response is the per-unit cost multiplied by the number of units required to achieve a given level of service. For example, using the per-unit cost of \$1.15 from Section 3.2, meeting the national FRR using GSLs in heat pumps would require $(13.2 \text{ M}) * (\$1.15) = \15.2 M . A cost-benefit analysis of GSLs that compares these costs to current market values is presented in Subedi et al. (2023). Using their lower bound estimate of \$1/MWh of frequency response, the lifetime value of a single device ranges from \$4 for refrigerators to \$53 for EV chargers, depending on the device’s energy consumption and lifetime.

We note that this analysis assumes that the load profile for a given end use is constant so that a set of GSLs can provide a constant amount of frequency response over time. Although this might be appropriate for refrigerators, EV charging and HVAC profiles are not constant due to diurnal and seasonal variations in weather and occupant behavior. Figure 15 shows the projected daily load profile for Level 2 and Level 3 chargers in Texas and across the United States in 2030 (Wood et al. 2023). EV chargers would provide significantly less frequency response when EV charging loads are low. This issue could be mitigated by using other devices during these times. For example, VRE sources could provide up-frequency response during times of low load because curtailment is likely to be more economic (and occasionally necessary) at these times.

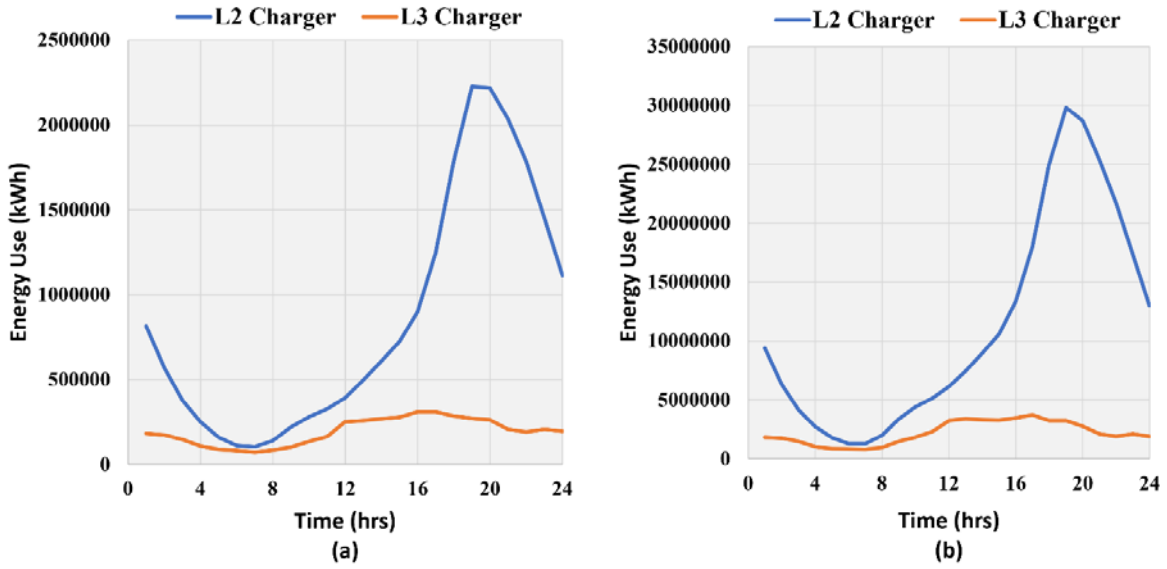


Figure 15. Baseline load profile estimation of Level 2 and Level 3 EV chargers by 2030 in (a) Texas and (b) the contiguous United States

Source: Image from NREL. Based on preliminary results from Wood et al. 2023

5 Conclusion

GSLs are power electronics-based end-use loads that can provide frequency response by autonomously adjusting the power of variable-speed and variable-power loads. As the integration of VRE sources and other inverter-based resources increases, the inertia of the electric grid decreases, and there is an increasing need for frequency response. GSLs can be a cost-effective option for up-frequency response in a low-inertia grid because they have low operational costs relative to other resources and have minimal impact on the end user. Given the rapidly changing mix of electric grid generators and loads, it is difficult to predict whether GSLs will be a cost-effective resource for frequency response and other grid services.

This report describes hardware designs and costs associated with implementing GSL functions in end-use loads. Five hardware implementation designs with different line frequency measurement circuits and isolators are analyzed for single- and three-phase devices. We assess each design in terms of materials, costs, and impacts on isolation and microcontroller requirements, and we estimate the energy consumption associated with GSL functionality. We find that the Type V design with the optocoupler is the most cost-effective design for GSL implementation with signal isolation. The additional cost incurred for this design is \$1.15 for single-phase loads and \$2.46 for the three-phase loads. We find that the energy loss from the GSL hardware is low; energy losses of 0.29% are estimated for refrigerators, and smaller losses are expected for other loads with higher energy consumption. Additional cost reductions and efficiency improvements are likely in many devices if GSL hardware can use existing voltage sensing circuits and microcontrollers.

We show that, if implemented at scale, GSLs can provide a significant amount of the current frequency response requirements in U.S. grids. Millions of refrigerators, EV chargers, or residential heat pumps would be required to meet 100% of the current national requirement, which is feasible given the number of available devices on the grid by 2030. We list the technical and market barriers associated with GSLs, and we describe multiple adoption pathways to mitigate these barriers and encourage GSL growth.

This report presents analysis on the feasibility and practicality of implementing GSLs in real systems; however, more research is needed before piloting GSLs on electric grids. We are planning a lab demonstration to assess the performance of GSL hardware in real devices. This work will measure the grid benefits of GSLs under various control methods as well as the impacts on the device and the user. Developing standards for GSL controls and performance is another important next step before implementing GSL functionality in products at scale.

References

- Anderson, Benjamin, Jim Reilly, and Venkat Krishnan. 2022. *Load Control for Frequency Response - A Literature Review*. Golden, CO: National Renewable Energy Laboratory. NREL/TP-5000-77780. <https://doi.org/10.2172/1846936>.
- Bhardwaj, Manish, and Jongwan Kim. 2021. “Bidirectional Interleaved CCM Totem Pole Bridgeless PFC RefDesign C2000 MCU.” Texas Instruments. April 2021. <https://www.ti.com/tool/TIDM-1007#applications>.
- Blonsky, Michael, Sunil Subedi, and Barry Mather. 2022. “Assessing the Technical Potential of Fast Frequency Response in Grid-Supportive Loads.” Presented at the IEEE PES General Meeting, Denver, CO, July 17, 2022. Golden, CO: National Renewable Energy Laboratory. <https://www.osti.gov/biblio/1878125>.
- Bonifield, Tom. 2017. *Enabling High Voltage Signal Isolation Quality and Reliability*. Dallas, TX: Texas Instruments. <https://www.ti.com/lit/wp/sszy028/sszy028.pdf>.
- California Public Utilities Commission. 2017. “Rule 21 Interconnection.” Rule 21 Working Group. <https://www.cpuc.ca.gov/rule21/>.
- Chakravorty, Diptargha, Balarko Chaudhuri, and Shu Yuen Ron Hui. 2017. “Rapid Frequency Response From Smart Loads in Great Britain Power System.” *IEEE Transactions on Smart Grid* 8 (5): 2160–69. <https://doi.org/10.1109/TSG.2016.2517409>.
- Denholm, Paul, Douglas J. Arent, Samuel F. Baldwin, Daniel E. Bilello, Gregory L. Brinkman, Jaquelin M. Cochran, Wesley J. Cole, et al. 2021. “The Challenges of Achieving a 100% Renewable Electricity System in the United States.” *Joule* 5 (6): 1331–52. <https://doi.org/10.1016/j.joule.2021.03.028>.
- Denholm, Paul, Trieu Mai, Richard Wallace Kenyon, Benjamin Kroposki, and Mark O’Malley. 2020. *Inertia and the Power Grid: A Guide Without the Spin*. NREL/TP-6A20-73856. Golden, CO: National Renewable Energy Laboratory. <https://doi.org/10.2172/1659820>.
- Denholm, Paul, Yinong Sun, and Trieu T. Mai. 2019. *An Introduction to Grid Services: Concepts, Technical Requirements, and Provision from Wind*. NREL/TP-6A20-72578. Golden, CO: National Renewable Energy Laboratory. <https://doi.org/10.2172/1493402>.
- EIA. 2020. “U.S. Energy Information Administration (EIA) - 2020 Residential Energy Consumption Survey (RECS) Data.” <https://www.eia.gov/consumption/residential/data/2020/#appliances>.
- Ela, Erik, Robin Broder Hytowitz, and Udi Helman. 2019. *Ancillary Services in the United States: Technical Requirements, Market Designs, and Price Trends*. EPRI: Palo Alto, CA, USA.
- ENERGY STAR. 2021. “The U.S. Environmental Protection Agency (EPA) - 2020-2021 Advanced Adaptive Compressors.” 2021. https://www.energystar.gov/about/awards/energy_star_emerging_technology_award_consumers/2020_advanced_adaptive_compressors.
- Gong, Xun, and Jayanth Rangaraju. 2018. *Taking Charge of Electric Vehicles-Both in the Vehicle and on the Grid*. Dallas, TX: Texas Instruments.
- Hoke, Anderson F., Austin A. Nelson, Jin Tan, Rasel Mahmud, Vahan Gevorgian, Mohamed Elkhatib, Chris Antonio, Dean Arakawa, and Ken Fong. 2017. *The Frequency-Watt Function: Simulation and Testing for the Hawaiian Electric Companies*. NREL/TP-5D00-68884. Golden, CO: National Renewable Energy Laboratory. <https://doi.org/10.2172/1373491>.

- IEEE. 2018. IEEE Std. 1547-2018 - IEEE Standard for Interconnection and Interoperability of Distributed Energy Resources with Associated Electric Power Systems Interfaces. <https://doi.org/10.1109/IEEESTD.2018.8332112>.
- Jain, Himanshu, Barry Mather, Akshay Kumar Jain, and Samuel F. Baldwin. 2022. “Grid-Supportive Loads—A New Approach to Increasing Renewable Energy in Power Systems.” *IEEE Transactions on Smart Grid* 13 (4): 2959–72. <https://doi.org/10.1109/TSG.2022.3153230>.
- Johnson, Samuel C., Joshua D. Rhodes, and Michael E. Webber. 2020. “Understanding the Impact of Non-Synchronous Wind and Solar Generation on Grid Stability and Identifying Mitigation Pathways.” *Applied Energy* 262 (March): 114492. <https://doi.org/10.1016/j.apenergy.2020.114492>.
- Jorgenson, Jennie L., and Paul L. Denholm. 2019. *Modeling Primary Frequency Response for Grid Studies*. NREL/TP-6A20-72355. Golden, CO: National Renewable Energy Laboratory. <https://doi.org/10.2172/1489895>.
- Kamath, Anant S. 2015. “Isolation in AC Motor Drives: Understanding the IEC 61800-5-1 Safety Standard.” Dallas, TX: Texas Instruments.
- Kliger, R. 2003. “Integrated Transformer-Coupled Isolation.” *IEEE Instrumentation & Measurement Magazine* 6 (1): 16–19. <https://doi.org/10.1109/MIM.2003.1184271>.
- Kulkarni, Abhijit, and Vinod John. 2013. “A Novel Design Method for SOGI-PLL for Minimum Settling Time and Low Unit Vector Distortion.” In *IECON 2013 - 39th Annual Conference of the IEEE Industrial Electronics Society*, 274–79. <https://doi.org/10.1109/IECON.2013.6699148>.
- Lundstrom, Blake, Sourav Patel, and Murti V. Salapaka. 2021. “Distribution Feeder-Scale Fast Frequency Response via Optimal Coordination of Net-Load Resources—Part I: Solution Design.” *IEEE Transactions on Smart Grid* 12 (2): 1289–1302. <https://doi.org/10.1109/TSG.2020.3032097>.
- Mai, Trieu T., Paige Jadun, Jeffrey S. Logan, Colin A. McMillan, Matteo Muratori, Daniel C. Steinberg, Laura J. Vimmerstedt, Benjamin Haley, Ryan Jones, and Brent Nelson. 2018. *Electrification Futures Study: Scenarios of Electric Technology Adoption and Power Consumption for the United States*. Golden, CO: National Renewable Energy Laboratory.
- Maniar, Krunal. 2019. *Comparing Isolated Amplifiers and Isolated Modulators*. Dallas, TX: Texas Instruments. <https://www.ti.com/lit/wp/sbaa359a/sbaa359a.pdf>.
- McGrath, Glenn. 2021. “Battery Storage Applications Have Shifted as More Batteries Are Added to the U.S. Grid.” *Today in Energy*. November 1, 2021. <https://www.eia.gov/todayinenergy/detail.php?id=50176>.
- Nandanoori, Sai Pushpak, Soumya Kundu, Dragana Vrabie, Karan Kalsi, and Jianming Lian. 2018. “Prioritized Threshold Allocation for Distributed Frequency Response.” In *2018 IEEE Conference on Control Technology and Applications (CCTA)*, 237–44. <https://doi.org/10.1109/CCTA.2018.8511411>.
- NXP Semiconductors. 2022. “Refrigerator Compressor.” <https://www.nxp.com/design/designs/refrigerator-compressor:REFRIGERATOR-COMPRESSOR>.
- Present, Elaina K. 2019. “End Use Load Profiles for the U.S. Building Stock.” Presented at the Introducing End Use Load Profiles Study for the U.S. and Northeast Webinar, October 24, 2019. Golden, CO: National Renewable Energy Laboratory. NREL/PR-5500-75282. <https://www.osti.gov/biblio/1572770>.

- Present, Elaina, Philip R. White, Rajendra Adhikari, Noel Merket, Eric J.H. Wilson, and Anthony Fontanini. 2022. “End-Use Savings Shapes - Public Dataset Release for Residential Round 1.” Presented on September 20, 2022. <https://www.nrel.gov/buildings/assets/pdfs/euss-resround1-webinar.pdf>.
- Rao, Prakash, Paul Sheaffer, Yuting Chen, Miriam Goldberg, Benjamin Jones, Jeff Cropp, and Jordan Hester. 2021. *U.S. Industrial and Commercial Motor System Market Assessment Report Volume 1: Characteristics of the Installed Base*. Berkeley, CA: Lawrence Berkeley National Laboratory. <https://doi.org/10.2172/1760267>.
- Rodriguez, Pedro, Josep Pou, Joan Bergas, J. Ignacio Candela, Rolando P. Burgos, and Dushan Boroyevich. 2007. “Decoupled Double Synchronous Reference Frame PLL for Power Converters Control.” *IEEE Transactions on Power Electronics* 22 (2): 584–92. <https://doi.org/10.1109/TPEL.2006.8900000>.
- Sahasrabudhe, Shubham. 2019. “Zero-Crossing Detection with False Trigger Avoidance.” 2019. <https://www.ti.com/lit/an/sbaa356/sbaa356.pdf?ts=1677534913507>.
- Subedi, Sunil, Michael Blonsky, Yeongrack Son, and Barry Mather. 2023. “Cost-Benefit Analysis of Grid-Supportive Loads for Fast Frequency Response: Preprint.” To be presented at the IEEE PES Grid Edge Technologies Conference and Exposition, San Diego, CA, April 10-13, 2023. Golden, CO: National Renewable Energy Laboratory. NREL/CP-6A40-83405. <https://www.nrel.gov/docs/fy23osti/83405.pdf>.
- Subedi, Sunil, Robert Fourney, Hossein Moradi Rekabdarkolae, Reinaldo Tonkoski, Timothy M. Hansen, Jesus D. Vasquez-Plaza, and Fabio Andrade. 2022. “Impact of PLL Design on Data-Driven Models for Grid-Connected Single-Phase Inverters.” In *2022 International Symposium on Power Electronics, Electrical Drives, Automation and Motion (SPEEDAM)*, 930–35. <https://doi.org/10.1109/SPEEDAM53979.2022.9841972>.
- Wood, E., B. Borlaug, M. Moniot, D.-Y. Lee, Y. Ge, F. Yang, and Z. Liu. 2023. *50x30: Estimating U.S. Charging Needs Toward 50% Light-Duty Electric Vehicle Sales by 2030*. Golden, CO: National Renewable Energy Lab. NREL/TP-5400-85654.
- Yao, Wenxuan, Shutang You, Weikang Wang, Xianda Deng, Yicheng Li, Lingwei Zhan, and Yilu Liu. 2020. “A Fast Load Control System Based on Mobile Distribution-Level Phasor Measurement Unit.” *IEEE Transactions on Smart Grid* 11 (1): 895–904. <https://doi.org/10.1109/TSG.2019.2926205>.